

1 **Global Flash Droughts Characteristics: Onset, Duration and Extent at Watershed Scales**

2  
3 Maheshwari Neelam<sup>1,2</sup>, Christopher Hain<sup>2</sup>

4  
5 <sup>1</sup> Universities Space Research Association, Huntsville, AL 35801, USA

6 <sup>2</sup> NASA Marshall Space Flight Center, Earth Science Branch, Huntsville, AL 35801,  
7 USA

8  
9 Corresponding author: Maheshwari Neelam (maheshwari.neelam@nasa.gov)

10  
11  
12 **Key Points:**

- 13
- 14 • The onset and duration of flash droughts at the watershed scale are influenced by climate  
15 variables, but not by the length of wet and dry spell.
  - 16 • Flash droughts extents are affected by intraannual precipitation variability, but not by  
17 intraannual air temperature variability.
  - 18 • Watersheds in tropical, temperate climates, and with savanna and grassland land cover  
19 are more susceptible to flash droughts.
- 20  
21  
22  
23  
24  
25  
26  
27  
28  
29

# Global Flash Droughts Characteristics: Onset, Duration and Extent at Watershed Scales

Maheshwari Neelam, Christopher Hain

## Abstract

Addressing impacts of flash droughts (FDs) on the water-food nexus requires a understanding of FD mechanisms and drivers at the watershed level. Examining climatic drivers, dry and wet spell lengths from 1980 to 2019 using long term MERRA-2 reanalysis data, we analyzed FD spatial and temporal characteristics, emphasizing areal extent, onset time, and duration. Our findings reveal substantial variations in FDs among different watersheds. Notably, watersheds in the Southern Hemisphere are witnessing expanding, faster-developing, and longer-lasting FDs, aligning with climate variations in precipitation and temperature. Additionally, at the watershed scale, the onset and duration of FDs are significantly more influenced by the intensity of climatic drivers than the duration of wet and dry periods. FD-extents, however, correlate with both climatic conditions and wet and dry periods, underscoring watershed connectivity. Ultimately, our results underscore the necessity for research to comprehend the interplay between FDs and watershed characteristics and how it manifests in overall water resource management.

## Plain Language Summary

Flash droughts (FDs), which are sudden and severe dry periods, are causing problems for our water and food systems and making it harder to prepare for disasters. To address these challenges effectively, it is crucial to gain a thorough understanding of the underlying mechanisms and factors driving FDs at the watershed level. In this study, we looked at climatic patterns alongside the lengths of dry and wet periods spanning from 1980 to 2019. Our primary focus was on three key aspects: the extent of FDs, when they begin, and how long they persist. Our research findings demonstrate considerable variations in FDs occurrences across different regions. Notably, in the Southern Hemisphere, FDs are expanding rapidly, developing more swiftly, and enduring for extended periods, closely mirroring shifts in precipitation and temperature patterns. Interestingly, the onset and duration of FDs seem to depend more on the intensity of climatic

60 factors than on how long it's been dry or wet. The expansion of FDs in a region is linked to both  
61 the climatic and dry/wet periods, emphasizing the geophysical connectivity within a watershed.

62

63

64

65

66

67 **1. Introduction**

68 Droughts are often described as "creeping hazards" due to their indefinite start and end  
69 times, encompassing wide spatial ranges (from a few kilometers to regional scales) and temporal  
70 footprints (spanning from weeks and months to even years) (Svoboda et al., 2002). Among these,  
71 flash droughts (FDs) stand out as a distinct category, marked by their rapid onset and  
72 intensification often over a matter of days to few weeks (Mo and Lettenmaier, 2016; Tyagi et al.,  
73 2022; Christian et al., 2021a; Christian et al., 2021b). This unique characteristic renders them  
74 more challenging to anticipate and address compared to traditional droughts. For example, FDs  
75 in the Dakotas and Montana in 2017 led to \$2.6 billion in agricultural losses in the U.S. alone  
76 (Basara et al., 2023). Recent years have witnessed a surge in research dedicated to understanding  
77 FDs, given the escalating challenges they pose. However, consensus remains elusive within the  
78 scientific community regarding a singular, universally accepted definition for this complex  
79 phenomena (Mo and Lettenmaier, 2015; Mo and Lettenmaier, 2016; Ford and Labosier, 2017;  
80 Chen et al., 2019; Koster et al., 2019; Pendergrass et al., 2020; Christian et al., 2021a; Christian  
81 et al., 2021b). Moreover, there is a range of indices available to identify FDs, including the  
82 Evaporative Demand Drought Index (EDDI) (Hobbins et al., 2016), the Evaporative Stress Index  
83 (ESI) (Otkin et al., 2014), the Standard Evaporative Stress Ratio (SESR) (Christian et al., 2019),  
84 and combinations of climate variables such as precipitation, air temperature, soil moisture, root-  
85 zone soil moisture, vapor pressure deficit, evapotranspiration and vegetation greenness.  
86 However, root zone soil moisture is key variable to several of these FD definitions, due to its  
87 relevance to vegetation and low noise relative to soil moisture, precipitation and temperature  
88 (Osman et al., 2021). Within the various definitions proposed, Christian et al., 2019 uses the ratio  
89 between evapotranspiration and potential evapotranspiration, while Otkin et al., 2018 uses  
90 intensification of an index (like evapotranspiration) accompanied by declining soil moisture.  
91 Conversely, Ford and Labosier, 2017 and Koster et al., 2019b, define it as a drop in root zone  
92 soil moisture from the 40<sup>th</sup> to below the 20<sup>th</sup> percentile over a 20-day span. This delineates the  
93 upper threshold as indicative of non-drought soil moisture conditions, while the lower threshold  
94 corresponds to the definition of moderate drought as per the U.S. Drought Monitor (USDM;  
95 Svoboda et al., 2002). Chen et al., 2019, base their definition on the USDM and its association  
96 with cold ENSO events. Similarly, Pendergrass et al., 2020 define FDs through rapid shifts in  
97 USDM categories, while Mo and Lettenmaier (2015, 2016) categorize them based on triggering

98 factors: heatwaves and precipitation deficits. However, in aiding the identification and  
99 conceptualization of FDs, studies have postulated three overarching principles:

- 100 • **Rapid onset:** FDs should initiate within days to a few weeks, distinguishing them from  
101 the gradual development of conventional droughts.
- 102 • **Intensification:** The severity of the drought should escalate rapidly, allowing for a  
103 transition from moderate to severe drought within a short timeframe.
- 104 • **Severity of impact:** The ultimate outcome of the event should be sufficiently severe to  
105 classify it as a FD.

106 It's important to note that these principles are not intended as rigid definitions but rather as  
107 foundational elements for developing quantitative metrics that facilitate early detection and  
108 mitigation of FDs. FDs induced from elevated air temperatures intensifying evapotranspiration  
109 and depleting root zone soil moisture. Conversely, FDs stemming from precipitation deficits  
110 cause a decline in root zone soil moisture due to insufficient water to wet the rootzone. Thus,  
111 FDs are a result of the interplay between factors like precipitation deficits and heightened air  
112 temperatures driving increased evapotranspiration (Mo and Lettenmaier, 2015; Mo and  
113 Lettenmaier, 2016; Koster 2019; Pendergrass et al., 2020; Christian et al., 2021a; Christian et al.,  
114 2021b). Beyond precipitation deficits and elevated evapotranspiration demand, an array of other  
115 environmental drivers can either amplify or alleviate the occurrence of FDs. These encompass  
116 factors like wet/dry spell, solar radiation, relative humidity, groundwater availability, soil water  
117 holding capacity, presence of organic matter, and vegetation cover. Notably, vegetation plays a  
118 significant role in modulating the rate of evapotranspiration and can expedite the onset of FDs  
119 (Ahmad et al., 2022). In general, vegetation cover influences evaporation and transpiration  
120 through precipitation interception, soil shading, and controlled stomatal conductance.

121 While many studies have explored the impact of climate drivers on FDs at a global scale  
122 providing valuable insights into global trends, only a limited number (Van Loon and Laaha,  
123 2015; Konapala and Mishra, 2020) have delved into the specifics of FDs within particular  
124 watersheds. Beyond climatic factors, the variability in watershed characteristics plays a  
125 substantial role in shaping the spatiotemporal dynamics of FD characteristics, which were  
126 overlooked in these studies. The objective of this study is to conduct a quantitative analysis of  
127 FD characteristics, climatic drivers, and the durations of wet and dry spells at the watershed level  
128 on a global scale, with a particular emphasis on FD spatial expansions. The findings compel the

129 introduction of a map specifically designed to assess FD vulnerability, which identifies hotspots  
130 undergoing one, two or three of these FD characteristics: the rate of change in area coverage,  
131 timeframes associated with FD-onset, and duration. The map highlights regions with  
132 susceptibility to future droughts, which may be prone to further cascading and compounding  
133 disasters.

## 134 **2. Data and Methodology**

### 135 **2.1. Study Area**

136 The analysis is conducted globally at a watershed scale to gain insights into the dynamics  
137 of FD characteristics and the factors driving them. The watershed characteristics, like pooling,  
138 attenuation, lag, and lengthening, play a pivotal role in shaping the hydrological responses  
139 (Eltahir and Yeh, 1999; Van Lanen et al., 2013). Lag time, for instance, measures the speed of a  
140 watershed's response to a runoff-producing rain event. These characteristics significantly impact  
141 various aspects of the hydrological cycle, influencing root zone soil moisture, subsurface  
142 recharge, and flow patterns. The variability in watershed attributes significantly contributes to  
143 the intricate interactions affecting FD propagation, duration, and their implications for the overall  
144 water balance (Van Loon and Laaha, 2015; Konapala and Mishra, 2020). It's important to note  
145 that while this study doesn't explicitly consider specific watershed characteristics, the analysis of  
146 FD at the watershed level inherently encompasses their influence as a significant driving factor  
147 in shaping distinct FD attributes.

### 148 **2.2. Data Description**

149 The focus of this study is on the warm season, which is from mid-April to mid-September  
150 in the Northern Hemisphere and from mid-October to mid-March in the Southern Hemisphere.  
151 We use Modern-Era Retrospective analysis for Research and Applications Version-2 (MERRA-  
152 2) (Gelaro et al., 2017), a state-of-the-art, multiyear atmospheric reanalysis product developed by  
153 NASA's Global Modeling and Assimilation Office (GMAO). MERRA-2 blends satellite and  
154 more conventional weather observations with model outputs to produce atmospheric and land  
155 variables. MERRA-2 fields are gridded hourly at a  $0.625^\circ$  longitude  $\times$   $0.5^\circ$  latitude resolution.  
156 The advantage of a reanalysis product is that it provides both spatial and temporal coherence for  
157 many climate variables, making it highly valuable for studying spatial trends over long periods  
158 of time, especially droughts. The accuracy of MERRA-2 fields has been validated extensively  
159 (Reichle et al., 2017). The rootzone soil moisture (RZSM) obtained from MERRA-2 is model-

160 generated, relying on atmospheric forcings, soil properties, and model parameterizations.  
161 However, given the specific focus of our analysis, MERRA-2 reanalysis emerges as the optimal  
162 choice for obtaining RZSM among other datasets (Liu et al., 2023). For this analysis, the  
163 MERRA-2 daily fields of RZSM ( $\text{m}^3/\text{m}^3$ ) precipitation ( $P$ ) (mm/day), total evapotranspiration  
164 (ET) (mm/day), sensible heat flux (SH) ( $\text{W}/\text{m}^2$ ), latent heat flux (LH) ( $\text{W}/\text{m}^2$ ), and 2-m air-  
165 temperature ( $T_{\text{air}}$ ) (K) from 1980 – 2019 are used. We also consider factors such as wet spell  
166 length which is defined as the number of consecutive days with  $P > 1\text{mm}$ , and dry spell length  
167 which refers to the number of days with no  $P$ . These durations of wet and dry spells play a  
168 significant role in influencing the moisture levels in the root zone.

### 169 **2.3. Flash Drought Definition**

170 In this study, we adopt the broad definition of FDs as established in Koster et al., 2019b,  
171 while diverging from their specific requirement that FDs exclusively develop over a 20-day  
172 period. The development of FDs varies across regions due to distinct geographical, climate and  
173 land cover factors. Instead our approach accommodates a variable development timescales for  
174 FDs, ranging from 15 to 45 days. Events that develop in less than 15 days are classified as mere  
175 water deficit. While there is no universally accepted timescale for FD duration (FD-Dur), we  
176 consider any event longer than 30 days as a hydrological drought. To identify FDs, we construct  
177 a cumulative distribution function (CDF) of RZSM at a specific location “j” and on a given day  
178 of the year “k”. This CDF is based on RZSM from 200 values from days “k – 6,” “k – 3,” “k,” “k  
179 + 3,” and “k + 6,” extracted from 1980 – 2019. This methodology offers several advantages,  
180 including its ability to effectively capture regional disparities and seasonal variations in the  
181 developed CDF. Moreover, the use of five additional sampling dates enhances data quality and  
182 helps mitigate noisy fluctuations when estimating RZSM percentiles. We employ a single,  
183 hydrology-based quantitative metric and dataset to identify FDs, acknowledging that different  
184 definitions and datasets could yield different results. Therefore, a FD is identified by;

- 185 • A decline in RZSM from above its 40<sup>th</sup> percentile to below its 20<sup>th</sup> percentile value.
- 186 • Simultaneously, there must be a reduction in ET from at least 4/5<sup>th</sup> of the climatological  
187 ET to 3/5<sup>th</sup> or lower of the climatological ET.
- 188 • The duration of the FD is considered the period starting when RZSM falls below the 20<sup>th</sup>  
189 percentile and ending when it monotonically rises back above the 20<sup>th</sup> percentile.
- 190 • To avoid overlapping events, only one FD event is considered within a given year.

191 This study primarily examines three FD characteristics: extent, onset, and duration:

192 • **FD-onset:** Measures the speed of FD development.

193 • **FD-Dur:** Measures the duration of FDs.

194 • **FD-extent:** Measures the expansion of FDs.

195 The FD-onset and FD-Dur are computed for each gridded pixel and subsequently aggregated to  
196 the watershed scale. We specifically focus on watersheds where at least 20 % of the area is  
197 undergoing FD characteristics. Likewise, FD-extent is determined by the number of pixels  
198 identified as FD relative to the total number of pixels in the watershed. A 40-year time series of  
199 the aggregated FD characteristics at watershed scale undergoes a linear trend analysis to  
200 ascertain the rate (slope of the trend), and only statistical significance trends ( $p < 0.1$ ) are  
201 reported. While, the relationships between climate and FD characteristics are reported using  
202 Spearman correlation coefficients ( $p < 0.1$ ). We consider both the mean and standard deviation  
203 (std) for all climatic variables specific to the analysis period to understand inter and intra-annual  
204 variations on FD characteristics. Furthermore, we assess the spatial variability of these drivers  
205 particularly in relation to driving FD-extent within the watersheds using coefficient of variation  
206 (CV).

207

## 208 **3. Results and Discussions**

### 209 **3.1. Global Hotspots and Trends in Flash Droughts**

210 The average FD-onset time falls within a range of  $\sim 17.23$  to  $\sim 28.72$  days, while the  
211 average FD-Dur spans from  $\sim 3.65$  to  $\sim 21.09$  days. It's worth noting that FDs exhibit both  
212 spatial expansion and contraction trends, Fig.1. Particularly, FDs in the Southern Hemisphere are  
213 expanding and intensifying more rapidly, as well as lasting for longer durations, compared to  
214 FDs in the Northern Hemisphere. While most watersheds are experiencing expansion in FD-  
215 extent, those in Central Asia are witnessing a reduction in FD-extent. However, globally on  
216 average, the rate of FD-extent expansion surpasses the rate of FD-extent reduction. This  
217 expansion can be attributed to a combination of below-average  $P$  and higher  $T_{\text{air}}$  anomalies,  
218 which contribute to rapid RZSM depletion. On the other hand, the shrinkage in FD-extent may  
219 result from not only increased mean  $P$  but also from greater water availability due to rising  $T_{\text{air}}$   
220 in high mountain areas, which advance the timing of snowmelt and alter hydrological processes.  
221 A noteworthy finding is that, despite an increase in the average duration of wet spells, there has  
222 been a substantial reduction in both the mean and std of  $P$  on a global scale. This implies that  
223 there might not be a sufficient amount of  $P$  to adequately percolate and saturate the RZSM,  
224 which is essential for averting FD events. Additionally, there has been a global increase in the  
225 duration of dry spells.

### 226 **3.1.1. South America**

227 In South America, many watersheds exhibit all three FDs characteristics, making them  
228 hotspots. However, the rates of change and responses to climatic drivers vary across watersheds.  
229 Notably, FDs are developing more rapidly by an average of  $\sim 0.12$  day/year, and persist longer  
230 by  $\sim 0.15$  day/year, particularly in the southern parts of Brazil. The overall FD-extent in South  
231 America is increasing by  $\sim 3\%$  per year. Brazil which covers more than  $\sim 40\%$  of the  
232 Amazonian watershed, has an average FD-onset of  $\sim 21.95$  days and FD-Dur of  $\sim 14.97$  days.  
233 The key drivers of FD characteristics in this region include  $P$  deficit, elevated  $T_{\text{air}}$ , and shorter  
234 wet spells. These findings align with the concept of a heat-drought-heat cascade, where higher  
235  $T_{\text{air}}$  levels elevate SH, subsequently leading to further  $T_{\text{air}}$  increases. This rise in  $T_{\text{air}}$ , intensifies  
236 evaporative demand resulting in increased desiccation of soils and vegetation, consistent with  
237 previous findings (Jimenez et al., 2018; Wunderling et al., 2022; Papastefanou et al., 2022). FD  
238 trends in the Amazonian watershed are consistent with deforestation patterns in the region (Staal  
239 et al., 2020). The local ET contributes  $\sim 20\%$  to  $\sim 45\%$  of the total  $P$  over the Amazonian  
240 region (Burde et al., 2006; Staal et al., 2018). Consequently, increased deforestation disrupts

241 local coupling and atmospheric circulation through land–atmosphere feedbacks (Goessling and  
242 Reick, 2011) These changes further impact  $P$  deficits and lead to higher  $T_{\text{air}}$  anomalies.

243 Our study further reveals that the expanding extent of FDs in the Amazon region is  
244 significantly influenced by CV in wet periods within the watershed. This finding is consistent  
245 with our understanding that a higher CV in wet spells within a watershed provides adequate time  
246 for percolation, facilitating subsurface and RZSM recharge. This enhances watershed  
247 connectivity, influences runoff patterns, and impacts streamflow responses. However, this  
248 process is nonlinear due to watershed heterogeneity in factors such as vegetation, soil types, and  
249 elevation variations (Singh et al., 2021). Therefore, the expanding extent of FDs in South  
250 American watersheds can be attributed to a combination of  $P$  deficit, higher  $T_{\text{air}}$ , shorter wet  
251 periods, and reduced spatial variability in wet periods.

### 252 **3.1.2. Central Africa**

253 Many watersheds across Africa are experiencing all three FD characteristics, akin to  
254 South America, marking them hotspots. This pattern is particularly evident in countries such as  
255 Congo, Angola, Zambia, Zimbabwe, South Africa, Lesotho, and Madagascar. These findings  
256 raise concerns that these regions may be entering a prolonged drought phase. The expansion of  
257 FDs in Africa is significantly influenced by a number of factors, including declining mean  $P$ , std  
258  $P$ , higher mean  $T_{\text{air}}$  and SH, Fig.1. Additionally, both wet and dry spell periods play a role in  
259 FD-extent, in contrast to South America. These drivers have undergone substantial changes over  
260 the past four decades in the African region. For example, mean  $T_{\text{air}}$  has exhibited a consistent  
261 rise, increasing at a rate of  $\sim 0.03^{\circ}\text{K}/\text{year}$ , while mean  $P$  has been on a declining trend at a rate of  
262  $\sim 0.02 \text{ mm}/\text{year}$ . Furthermore, wet spells have been contracting by  $\sim 0.1 \text{ day}/\text{year}$ , while dry  
263 spells have been extending by  $\sim 0.04 \text{ day}/\text{year}$ . These findings are consistent with previous  
264 research that has documented a surge in temperatures and the emergence of more intense and  
265 prolonged heatwaves across various African regions (Russo et al., 2016; Ceccherini et al., 2017;  
266 Engdaw et al., 2022).

267 African watersheds face unique challenges due to their relatively arid nature compared to  
268 South American or Asian watersheds. As a result, African vegetation may already be operating  
269 close to its physiological and ecological limits (Bennett et al., 2021). Additionally,  $\sim 50 \%$  of  
270 Africa’s rainfall originates from vegetation sources within watersheds. However, the reliance on  
271 vegetation-sourced  $P$  varies significantly among different watersheds, ranging from  $\sim 5 \%$  to  $\sim$

272 68 % (Te Wierik et al., 2022). Any further temperature increases could result in a rapid  
273 escalation of ET from vegetation, further exacerbating the already arid conditions in Africa. This  
274 heightened sensitivity to  $T_{\text{air}}$  is also underscored by the strong correlation between the expansion  
275 of FD-extent and spatial variability in LH within the watershed. Additionally, FD-onset and FD-  
276 Dur are primarily driven by higher mean  $T_{\text{air}}$  and SH superseding the impact of mean  $P$ , Fig.2.  
277 In contrast to the Amazonian watersheds, FD-extent in African watersheds is influenced by the  
278 spatial CV of mean  $T_{\text{air}}$ , std  $T_{\text{air}}$ , and LH. This sets African watersheds apart from other regions.

### 279 3.1.3. Central Asia

280 Central Asian watersheds containing mountainous areas, including High Mountain Asia,  
281 Himalayan and the Tianshan Mountains, experience a noticeable reduction in FD-extent, with the  
282 strongest correlations with mean and std  $P$  and wet and dry spell lengths, Fig.1. However, FD-  
283 onset and FD-Dur show weak correlations with any drivers, Fig.2 (barplots). What sets this  
284 region apart is the contradictory nature of the trends in these drivers over the past four decades,  
285 in contrast to global patterns. For example, mean  $P$  has increased by  $\sim 0.03$  mm/year, along with  
286 an increase in std  $P$  by  $\sim 0.02$  mm/year. Additionally, wet spells have become longer by  $\sim 0.01$   
287 day/year, while dry spells have become shorter by  $\sim 0.05$  day/year. Although mean  $T_{\text{air}}$  has  
288 increased, it has done so at a slower rate than global trends. Our findings are consistent with  
289 other studies (Wang et al., 2016; Roxy et al., 2017) which observed an increase in  $P$  in  
290 mountainous areas of Central and East Asia since the 1980s. This may be due to the sensitivity of  
291 mountain snowpack to  $T_{\text{air}}$ , which influences the phase of  $P$ . Rising temperatures have also  
292 advanced snowmelt, increasing total surface water availability. This has led to changes in the  
293 timing and volume of river discharge, impacting the hydrology of the region (Maurer et al.,  
294 2019; Khanal et al., 2021). Mountainous areas are complex systems where runoff is a mix of  
295 rainfall, snowmelt, and glacier melt. A study by Nepal, 2016 found that glacier melt runoff  
296 contributes  $\sim 39$  % of streamflow during the monsoon season (June to September) in the  
297 Himalayan region. Nevertheless, the response to increase in  $T_{\text{air}}$  varies widely across different  
298 regions and elevations, depending on climate conditions (Blahušiaková et al., 2020). Despite the  
299 contrary characteristics of FDs in Central Asia compared to global trends, it continues to be  
300 recognized as a global hotspot and a region of heightened risk. This is because the fluctuations in  
301 climate and cryospheric conditions are expected to exacerbate snow droughts and events like

302 glacier outbursts and influence the seasonal water availability in downstream areas, potentially  
303 resulting in a heightened frequency of floods (Sattar et al., 2022; Taylor et al., 2023).

### 304 **3.2. Flash Drought Characteristics under Climate and Land Cover Classes**

305 Among the 30 Köppen climate classes (Beck et al., 2018), we observed notable changes  
306 in all three FD characteristics for Tropical Wet Savanna (Aw), Temperate (Cfb, Cfc), and  
307 Mediterranean (Csb) climates (Table 1). The most significant expansion in FD-extent is observed  
308 in the Aw climate class, indicating an annual increase of  $\sim 0.6\%$ . Our findings align with  
309 previous studies (Yuan et al., 2023) that have indicated regions with humid and semi-humid  
310 climates are more susceptible to FDs. When  $P$  deficits coincide with positive  $T_{\text{air}}$  anomalies, it  
311 intensifies atmospheric water demand, leading to accelerated SM depletion, particularly within  
312 these climate regions. Of the 15 International Geosphere–Biosphere Programme (IGBP) land  
313 cover classes, regions with Evergreen Broadleaf forests (EBFs) have experienced all three FD  
314 characteristics, and are expanding at  $\sim 0.39\%$  per year. EBFs maintain their foliage year-round  
315 and often do not shed leaves even during severe water deficits, which makes them more prone to  
316 drought (Anderson et al., 2018; Fu et al., 2013; Wang et al., 2016; Zhou et al., 2011). This is also  
317 likely due to a trend towards increased aridity and longer dry seasons in recent decades within  
318 EBFs (Boisier et al., 2015). Other land cover classes showing changes include Closed  
319 Shrublands, Savannas, Grasslands, and Croplands. FD-extent in Savannas are expanding, while  
320 FDs in other Grasslands are developing at a faster rate and lasting longer (Table. 1). This is  
321 similar to the findings of Wang et al., 2019, who ranked the impacts of drought on different  
322 grassland types as follows: Closed Shrublands, Non-woody grassland, Savannas, Open  
323 Shrublands, Woody Savannas. Although we observe accelerated FD-onset and longer FD-Dur in  
324 cropland regions, we do not find any evidence of expansion for FD-extent.

### 325 **3.3. Implications for Enhancing an Early Warning System**

326 It is well-established that disasters are not just natural occurrences, but also have social  
327 dimensions. Disasters happen when communities are not prepared for the consequences of  
328 natural hazards. Fortunately, there are many national and international early warning systems  
329 that can help identify emerging droughts, such as Climate Engine, the Drought Early Warning  
330 System, the Global Drought Information System etc., (Funk et al., 2019). However, FDs pose  
331 complex challenges for management and early warning systems because they can develop

332 rapidly. This rapid intensification of drought conditions reduces the lead time available for  
333 preparation and mitigation.

334         Recent research by Christian et al., 2023 shows that croplands are at risk of more  
335 frequent FDs, due to the influence of future climate change. Therefore, to support existing early  
336 warning systems, we present a vulnerability map based on four decades of historical data for  
337 watersheds that are prone to FDs and exhibiting one or combination of FD characteristics. The  
338 map (Fig.3) indicates the vulnerability of watersheds to future droughts, and thus their  
339 susceptibility to cascading and compounding disasters. Many of these regions, to say the least  
340 include Central America, Europe, Southeast Australia, Pakistan, and Central Africa, which have  
341 already experienced drought-related events such as flash floods, extreme heat, and wildfires.

#### 342 **4. Conclusions**

343         In this study, we conducted a comprehensive analysis of flash droughts (FDs) at the  
344 watershed scale, using 40 years of long-term reanalysis data to provide valuable insights into  
345 their spatial and temporal characteristics. We focused on three key aspects of FDs: their areal  
346 extent, onset time, and duration. Our findings revealed notable disparities in FD patterns among  
347 different watersheds. For instance, South American watersheds are currently experiencing the  
348 expansion and intensification of FDs. These trends primarily result from the dual impact of rising  
349 temperatures and declining precipitation. In the Central Africa watersheds, analogous  
350 vulnerabilities exist, but the influence of increasing temperatures outweighs diminishing  
351 precipitation in shaping FD characteristics. Conversely, Central Asian watersheds exhibit a  
352 mixed response in FD characteristics, largely driven by an unprecedented increase in  
353 precipitation. Climatic conditions and the lengths of wet and dry spells significantly affected FD-  
354 extent, underlining the geophysical connectivity within a watershed. Particularly noteworthy is  
355 the contrast between Southern Hemisphere and Northern Hemisphere watersheds, with the  
356 former experiencing FDs that expand more rapidly and endure longer, aligning with shifts in  
357 precipitation and temperature patterns. Furthermore, our analysis explored the roles of climate  
358 and land cover classes in shaping FD characteristics. Climates characterized as humid and semi-  
359 humid, such as Tropical Wet Savanna, displayed heightened susceptibility to FDs due to intricate  
360 interactions involving monsoons, temperature anomalies, and precipitation deficits. Land cover  
361 types such as Evergreen Broadleaf forests and Grasslands exhibited all three FD characteristics,  
362 emphasizing their vulnerability to prolonged drought conditions. Our findings can supplement

363 existing early warning systems and preparedness measures, especially in regions prone to FDs.  
364 As FDs can rapidly intensify, reducing the lead time available for mitigation, our vulnerability  
365 map based on historical data can aid in identifying regions susceptible to FDs and cascading  
366 disasters. Even though, our study is based on a specific hydrology-based FD definition and the  
367 use of MERRA-2 data, our primary aim was to comprehensively explore statistically significant  
368 rate-of-change trends in all three FD characteristics at the watershed scale globally, which is a  
369 novel approach that has not been undertaken in this manner before.  
370 While, the scalability of FD identification across datasets and definitions is beyond the scope of  
371 this study, it is recognized as a critical aspect that will be the subject of future research.

372

373

374

375

376 **Data Availability Statement:** The authors are thankful for the data provided by the  
377 Modern-Era Retrospective analysis for Research and Applications Version-2 developed by  
378 NASA's Global Modeling and Assimilation Office (GMAO).  
379 (<https://gmao.gsfc.nasa.gov/reanalysis/MERRA-2/>)

380  
381 **Acknowledgments:** This study was supported by the Short term Prediction and Transition  
382 Center (SPoRT) center of NASA MSFC. Additionally, the authors thank, Dr. Randal Koster and  
383 Dr. Benjamin Poulter for their insightful and valuable feedback.

384  
385  
386  
387  
388  
389  
390  
391  
392  
393  
394  
395 **References**

- 396 Ahmad, S. K., Kumar, S. V., Lahmers, T. M., Wang, S., Liu, P-W., Wrzesien, M. L., Bindlish,  
397 R., Getirana, A., Locke, K. A., Holmes, T. R., and Otkin, J. A. (2022). Flash Drought Onset and  
398 Development Mechanisms Captured With Soil Moisture and Vegetation Data Assimilation.  
399 *Water Resources Research*, 58(12), p.e2022WR032894.  
400  
401 Anderson, L. O., Ribeiro Neto, G., Cunha, A. P., Fonseca, M. G., Mendes de Moura, Y.,  
402 Dalagnol, R., Wagner, F. H., and de Aragão, L. E. O. E. C. (2018). Vulnerability of Amazonian  
403 forests to repeated droughts. *Philosophical Transactions of the Royal Society B: Biological*  
404 *Sciences*, 373(1760), p.20170411.  
405  
406 Ballesteros-Cánovas, J. A., Trappmann, D., Madrigal-González, J., Eckert, N., and Stoffel, M.  
407 (2018). Climate warming enhances snow avalanche risk in the Western Himalayas. *Proceedings*  
408 *of the National Academy of Sciences*, 115, 3410–5.  
409

410 Beck, H. E., Zimmermann, N. E., McVicar, T. R., Vergopolan, N., Berg, A., and Wood, E. F.  
411 (2018). Present and future Köppen-Geiger climate classification maps at 1-km resolution.  
412 *Scientific Data*, 5, 180214.

413

414 Bennett, A. C., Dargie, G. C., Cuni-Sanchez, A., Tshibamba Mukendi, J., Hubau, W., Mukinzi,  
415 J. M., Phillips, O. L., Malhi, Y., Sullivan, M. J. P., Cooper, D. L. M., Adu-Bredu, S., Affum-  
416 Baffoe, K., Amani, C. A., Banin, L. F., Beeckman, H., Begne, S. K., Bocko, Y. E., Boeckx, P.,  
417 Bogaert, J., Brncic, T., Chezeaux, E., Clark, C. J., Daniels, A. K., de Haulleville, T., Djuikouo  
418 Kamdem, M-N., Doucet, J-L., Evouna Ondo, F., Ewango, C. E. N., Feldpausch, T. R., Foli, E.  
419 G., Gonmadje, C., Hall, J. S., Hardy, O. J., Harris, D. J., Ifo, S. A., Jeffery, K. J., Kearsley, E.,  
420 Leal, M., Levesley, A., Makana, J-R., Mbayu Lukas, F., Medjibe, V. P., Mihindu, V., Moore,  
421 S., Nssi Begone, N., Pickavance, G. C., Poulsen, J. R., Reitsma, J., Sonké, B., Sunderland, T. C.  
422 H., Taedoumg, H., Talbot, J., Tuagben, D. S., Umunay, P. M., Verbeeck, H., Vleminckx, J.,  
423 White, L. J. T., Woell, H., Woods, J. T., Zemagho, L., and Lewis, S. L. (2021). Resistance of  
424 African tropical forests to an extreme climate anomaly. *Proceedings of the National Academy of*  
425 *Sciences*, 118, e2003169118.

426

427 Blahušáková, A., Matoušková, M., Jeníček, M., Ledvinka, O., Kliment, Z., Podolinská, J., and  
428 Snopková, Z. (2020). Snow and climate trends and their impact on seasonal runoff and  
429 hydrological drought types in selected mountain catchments in Central Europe. *Hydrological*  
430 *Sciences Journal*, 65, 2083–96.

431

432 Boisier, J. P., Ciais, P., Ducharne, A., and Guimberteau, M. (2015). Projected strengthening of  
433 Amazonian dry season by constrained climate model simulations. *Nature Climate Change*, 5,  
434 656–60.

435

436 Burde, G. I., Gandush, C., and Bayarjargal, Y. (2006). Bulk Recycling Models with Incomplete  
437 Vertical Mixing. Part II: Precipitation Recycling in the Amazon Basin. *Journal of Climate*, 19,  
438 1473–89.

439

440 Ceccherini, G., Russo, S., Ameztoy, I., Marchese, A. F., and Carmona-Moreno, C. (2017). Heat  
441 waves in Africa 1981–2015, observations and reanalysis. *Natural Hazards and Earth System*  
442 *Sciences*, 17, 115–25.

443

444 Chen, L. G., Gottschalck, J., Hartman, A., Miskus, D., Tinker, R., and Artusa, A. (2019). Flash  
445 Drought Characteristics Based on U.S. Drought Monitor. *Atmosphere*, 10, 498.

446

447 Christian, J. I., Basara, J. B., Otkin, J. A., Hunt, E. D., Wakefield, R. A., Flanagan, P. X., and  
448 Xiao, X. (2019). A methodology for flash drought identification: Application of flash drought  
449 frequency across the United States. *Journal of Hydrometeorology*, 20(5), pp.833-846.

450

451 Christian, J. I., Basara, J. B., Hunt, E. D., Otkin, J. A., Furtado, J. C., Mishra, V., Xiao, X., and  
452 Randall, R. M. (2021a). Global distribution, trends, and drivers of flash drought occurrence.  
453 *Nature Communications*, 12, 6330.

454

455 Christian, J. I., Basara, J. B., Hunt, E. D., Otkin, J. A., Furtado, J. C., Mishra, V., Xiao, X., and  
456 Randall, R. M. (2021b). Global distribution, trends, and drivers of flash drought occurrence.  
457 *Nature Communications*, 12, 6330.  
458

459 Christian, J. I., Basara, J. B., Otkin, J. A., and Hunt, E. D. (2019). Regional characteristics of  
460 flash droughts across the United States. *Environmental Research Communications*, 1, 125004.  
461

462 Christian, J. I., Martin, E. R., Basara, J. B., Furtado, J. C., Otkin, J. A., Lowman, L. E. L., Hunt,  
463 E. D., Mishra, V., and Xiao, X. (2023). Global projections of flash drought show increased risk  
464 in a warming climate. *Communications Earth & Environment*, 4, 1–10.  
465

466 Eltahir, E. A. B., and Yeh, P. J-F. (1999). On the asymmetric response of aquifer water level to  
467 floods and droughts in Illinois. *Water Resources Research*, 35, 1199–217.  
468

469 Engdaw, M. M., Ballinger, A. P., Hegerl, G. C., and Steiner, A. K. (2022). Changes in  
470 temperature and heat waves over Africa using observational and reanalysis data sets.  
471 *International Journal of Climatology*, 42, 1165–80.  
472

473 Feng, S., and Fu, Q. (2013). Expansion of global drylands under a warming climate.  
474 *Atmospheric Chemistry and Physics*, 13, 10081–94.  
475

476 Ford, T. W., and Labosier, C. F. (2017). Meteorological conditions associated with the onset of  
477 flash drought in the Eastern United States. *Agricultural and Forest Meteorology*, 247, 414–23.  
478

479 Funk, C., Shukla, S., Thiaw, W. M., Rowland, J., Hoell, A., McNally, A., Husak, G., Novella,  
480 N., Budde, M., Peters-Lidard, C., Adoum, A., Galu, G., Korecha, D., Magadzire, T., Rodriguez,  
481 M., Robjhon, M., Bekele, E., Arsenault, K., Peterson, P., Harrison, L., Fuhrman, S., Davenport,  
482 F., Landsfeld, M., Pedreros, D., Jacob, J. P., Reynolds, C., Becker-Reshef, I., and Verdin, J.  
483 (2019). Recognizing the Famine Early Warning Systems Network: Over 30 Years of Drought  
484 Early Warning Science Advances and Partnerships Promoting Global Food Security. *Bulletin of*  
485 *the American Meteorological Society*, 100, 1011–27.  
486

487 Fu, R., Yin, L., Li, W., Arias, P.A., Dickinson, R.E., Huang, L., Chakraborty, S., Fernandes, K.,  
488 Liebmann, B., Fisher, R., and Myneni, R.B. (2013). Increased dry-season length over southern  
489 Amazonia in recent decades and its implication for future climate projection. *Proceedings of the*  
490 *National Academy of Sciences*, 110(45), pp.18110-18115.  
491

492 Gelaro, R., McCarty, W., Suárez, M. J., Todling, R., Molod, A., Takacs, L., Randles, C. A.,  
493 Darmenov, A., Bosilovich, M. G., Reichle, R., Wargan, K., Coy, L., Cullather, R., Draper, C.,  
494 Akella, S., Buchard, V., Conaty, A., Silva, A. M. da, Gu, W., Kim, G-K., Koster, R., Lucchesi,  
495 R., Merkova, D., Nielsen, J. E., Partyka, G., Pawson, S., Putman, W., Rienecker, M., Schubert,  
496 S. D., Sienkiewicz, M., and Zhao, B. (2017). The Modern-Era Retrospective Analysis for  
497 Research and Applications, Version 2 (MERRA-2). *Journal of Climate*, 30, 5419–54.  
498

499 Goessling, H. F., and Reick, C. H. (2011). What do moisture recycling estimates tell us?  
500 Exploring the extreme case of non-evaporating continents. *Hydrology and Earth System*  
501 *Sciences*, 15, 3217–35.

502 Hobbins, M. T., A. Wood, D. J. McEvoy, J. L. Huntington, C. Morton, M. Anderson, and C.  
503 Hain (2016). The Evaporative Demand Drought Index. Part I: Linking drought evolution to  
504 variations in evaporative demand. *J. Hydrometeorol.*, 17, 1745–1761.

505

506 Immerzeel, W. W., Pellicciotti, F., and Bierkens, M. F. P. (2013). Rising river flows throughout  
507 the twenty-first century in two Himalayan glacierized watersheds. *Nature Geoscience*, 6, 742–5.

508 Jimenez, J. C., Libonati, R., and Peres, L. F. (2018). Droughts Over Amazonia in 2005, 2010,  
509 and 2015: A Cloud Cover Perspective. *Frontiers in Earth Science*, 6.

510

511 Khanal, S., Lutz, A. F., Kraaijenbrink, P. D. A., van den Hurk, B., Yao, T., and Immerzeel, W.  
512 W. (2021). Variable 21st Century Climate Change Response for Rivers in High Mountain Asia at  
513 Seasonal to Decadal Time Scales. *Water Resources Research*, 57, e2020WR029266.

514

515 Konapala, G., and Mishra, A. (2020). Quantifying Climate and Catchment Control on  
516 Hydrological Drought in the Continental United States. *Water Resources Research*, 56,  
517 e2018WR024620.

518

519 Konapala G and Mishra A (2020). Quantifying Climate and Catchment Control on Hydrological  
520 Drought in the Continental United States. *Water Resources Research*, 56, e2018WR024620.

521

522 Konapala, G., and Mishra, A. (2020). Quantifying Climate and Catchment Control on  
523 Hydrological Drought in the Continental United States. *Water Resources Research*, 56,  
524 e2018WR024620.

525

526 Koster, R. D., Schubert, S. D., Wang, H., Mahanama, S. P., and DeAngelis, A. M. (2019a). Flash  
527 Drought as Captured by Reanalysis Data: Disentangling the Contributions of Precipitation  
528 Deficit and Excess Evapotranspiration. *Journal of Hydrometeorology*, 20, 1241–58.

529

530 Koster, R. D., Schubert, S. D., Wang, H., Mahanama, S. P., and DeAngelis, A. M. (2019b). Flash  
531 Drought as Captured by Reanalysis Data: Disentangling the Contributions of Precipitation  
532 Deficit and Excess Evapotranspiration. *Journal of Hydrometeorology*, 20, 1241–58.

533

534 Liu, E., Zhu, Y., Calvet, J.C., Lü, H., Bonan, B., Zheng, J., Gou, Q., Wang, X., Ding, Z., Xu, H.  
535 and Pan, Y. (2023). Evaluation of model-derived root-zone soil moisture over the Huai river  
536 basin. *Hydrology and Earth System Sciences Discussions*, pp.1-39.

537

538 Lutz, A. F., Immerzeel, W. W., Shrestha, A. B., and Bierkens, M. F. P. (2014). Consistent  
539 increase in High Asia’s runoff due to increasing glacier melt and precipitation. *Nature Climate*  
540 *Change*, 4, 587–92.

541

542 Maurer, J. M., Schaefer, J. M., Rupper, S., and Corley, A. (2019). Acceleration of ice loss across  
543 the Himalayas over the past 40 years. *Science Advances*, 5, eaav7266.

544  
545 Mo, K. C., and Lettenmaier, D. P. (2015). Heat wave flash droughts in decline. *Geophysical*  
546 *Research Letters*, 42, 2823–9.  
547  
548 Mo, K. C., and Lettenmaier, D. P. (2016). Precipitation Deficit Flash Droughts over the United  
549 States. *Journal of Hydrometeorology*, 17, 1169–84.  
550  
551 Nepal, S. (2016). Impacts of climate change on the hydrological regime of the Koshi river basin  
552 in the Himalayan region. *Journal of Hydro-environment Research*, 10, 76–89.  
553  
554 Osman, M., Zaitchik, B. F., Badr, H. S., Christian, J. I., Tadesse, T., Otkin, J. A., and Anderson,  
555 M. C. (2021). Flash drought onset over the contiguous United States: sensitivity of inventories  
556 and trends to quantitative definitions. *Hydrology and Earth System Sciences*, 25(2), pp. 565-581.  
557  
558 Otkin, J. A., M. C. Anderson, C. Hain, and M. Svoboda. (2014). Examining the relationship  
559 between drought development and rapid changes in the Evaporative Stress Index. *Journal of*  
560 *Hydrometeorology*, 15, 938–956.  
561  
562 Otkin, J. A., Svoboda, M., Hunt, E. D., Ford, T. W., Anderson, M. C., Hain, C., and Basara, J. B.  
563 (2018). Flash Droughts: A Review and Assessment of the Challenges Imposed by Rapid-Onset  
564 Droughts in the United States. *Bulletin of the American Meteorological Society*, 99, 911–9.  
565  
566 Papastefanou, P., Zang, C. S., Angelov, Z., de Castro, A. A., Jimenez, J. C., De Rezende, L. F.  
567 C., Ruscica, R. C., Sakschewski, B., Sörensson, A. A., Thonicke, K., Vera, C., Viovy, N., Von  
568 Randow, C., and Rammig, A. (2022). Recent extreme drought events in the Amazon rainforest:  
569 assessment of different precipitation and evapotranspiration datasets and drought indicators.  
570 *Biogeosciences*, 19, 3843–61.  
571  
572 Pendergrass, A. G., Meehl, G. A., Pulwarty, R., Hobbins, M., Hoell, A., AghaKouchak, A.,  
573 Bonfils, C. J. W., Gallant, A. J. E., Hoerling, M., Hoffmann, D., Kaatz, L., Lehner, F.,  
574 Llewellyn, D., Mote, P., Neale, R. B., Overpeck, J. T., Sheffield, A., Stahl, K., Svoboda, M.,  
575 Wheeler, M. C., Wood, A. W., and Woodhouse, C. A. (2020). Flash droughts present a new  
576 challenge for subseasonal-to-seasonal prediction. *Nature Climate Change*, 10, 191–9.  
577  
578 Reichle, R. H., Draper, C. S., Liu, Q., Girotto, M., Mahanama, S. P. P., Koster, R. D., and  
579 Lannoy, G. J. M. D. (2017). Assessment of MERRA-2 Land Surface Hydrology Estimates.  
580 *Journal of Climate*, 30, 2937–60.  
581  
582 Roxy, M. K., Ghosh, S., Pathak, A., Athulya, R., Mujumdar, M., Murtugudde, R., Terray, P., and  
583 Rajeevan, M. (2017). A threefold rise in widespread extreme rain events over central India.  
584 *Nature Communications*, 8, 708.  
585  
586 Russo, S., Marchese, A. F., Sillmann, J., and Immé, G. (2016). When will unusual heat waves  
587 become normal in a warming Africa? *Environmental Research Letters*, 11, 054016.  
588

589 Sattar, A., Haritashya, U. K., Kargel, J. S., and Karki, A. (2022). Transition of a small  
590 Himalayan glacier lake outburst flood to a giant transborder flood and debris flow. *Scientific*  
591 *Reports*, 12, 12421.

592

593 Singh, N. K., Emanuel, R. E., McGlynn, B. L., and Miniati, C. F. (2021). Soil Moisture  
594 Responses to Rainfall: Implications for Runoff Generation. *Water Resources Research*, 57,  
595 e2020WR028827.

596

597 Staal, A., Flores, B. M., Aguiar, A. P. D., Bosmans, J. H. C., Fetzer, I., and Tuinenburg, O. A.  
598 (2020). Feedback between drought and deforestation in the Amazon. *Environmental Research*  
599 *Letters*, 15, 044024.

600

601 Staal, A., Tuinenburg, O. A., Bosmans, J. H. C., Holmgren, M., van Nes, E. H., Scheffer, M.,  
602 Zemp, D. C., and Dekker, S. C. (2018). Forest-rainfall cascades buffer against drought across the  
603 Amazon. *Nature Climate Change*, 8, 539–43.

604

605 Svoboda, M., LeCompte, D., Hayes, M., Heim, R., Gleason, K., Angel, J., Rippey, B., Tinker, R.,  
606 Palecki, M., and Stooksbury, D. (2002). The drought monitor. *Bulletin of the American*  
607 *Meteorological Society*, 83, 1181–90.

608

609 Taylor, C., Robinson, T. R., Dunning, S., Rachel Carr, J., and Westoby, M. (2023). Glacial lake  
610 outburst floods threaten millions globally. *Nature Communication*, 14, 487.

611

612 Te Wierik, S. A., Keune, J., Miralles, D. G., Gupta, J., Artzy-Randrup, Y. A., Gimeno, L., Nieto,  
613 R., and Cammeraat, L. H. (2022). The Contribution of Transpiration to Precipitation Over  
614 African Watersheds. *Water Resources Research*, 58, e2021WR031721.

615

616 Tyagi, S., Zhang, X., Saraswat, D., Sahany, S., Mishra, S. K., and Niyogi, D. (2022). Flash  
617 Drought: Review of Concept, Prediction and the Potential for Machine Learning, Deep Learning  
618 Methods. *Earth's Future*, 10, e2022EF002723.

619

620 Van Lanen, H. a. J., Wanders, N., Tallaksen, L. M., and Van Loon, A. F. (2013). Hydrological  
621 drought across the world: impact of climate and physical catchment structure. *Hydrology and*  
622 *Earth System Sciences*, 17, 1715–32.

623

624 Van Loon, A. F., and Laaha, G. (2015). Hydrological drought severity explained by climate and  
625 catchment characteristics. *Journal of Hydrology*, 526, 3–14.

626

627 Wang, W., Wang, J., Liu, X., Zhou, G., and Yan, J. (2016). Decadal drought deaccelerated the  
628 increasing trend of annual net primary production in tropical or subtropical forests in southern  
629 China. *Scientific Reports*, 6(1), p. 28640.

630

631 Wang, J., Zhang, M., Wang, S., Ren, Z., Che, Y., Qiang, F., and Qu, D. (2016). Decrease in  
632 snowfall/rainfall ratio in the Tibetan Plateau from 1961 to 2013. *Journal of Geographical*  
633 *Sciences*, 26, 1277–88.

634

635 Wang, Q., Yang, Y., Liu, Y., Tong, L., Zhang, Q., and Li, J. (2019). Assessing the Impacts of  
636 Drought on Grassland Net Primary Production at the Global Scale. *Scientific Reports*, 9, 14041.  
637  
638 Wunderling, N., Staal, A., Sakschewski, B., Hirota, M., Tuinenburg, O. A., Donges, J. F.,  
639 Barbosa, H. M. J., and Winkelmann, R. (2022). Recurrent droughts increase risk of cascading  
640 tipping events by outpacing adaptive capacities in the Amazon rainforest. *Proceedings of the*  
641 *National Academy of Sciences*, 119, e2120777119.  
642  
643 Yuan, X., Wang, Y., Ji, P., Wu, P., Sheffield, J. and Otkin, J.A.,(2023). A global transition to  
644 flash droughts under climate change. *Science*, 380(6641), pp.187-191.  
645  
646 Zhou, G., Wei, X., Wu, Y., Liu, S., Huang, Y., Yan, J., Zhang, D., Zhang, Q., Liu, J., Meng, Z.  
647 and Wang, C. (2011). Quantifying the hydrological responses to climate change in an intact  
648 forested small watershed in Southern China. *Global Change Biology*, 17(12), pp.3736-3746.  
649  
650  
651

Figure1.

### Rate of Change in Flash Drought Extent (percentage/year)

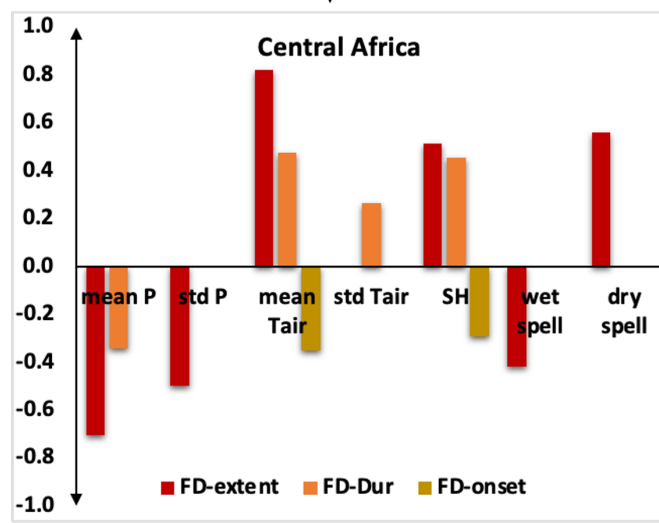
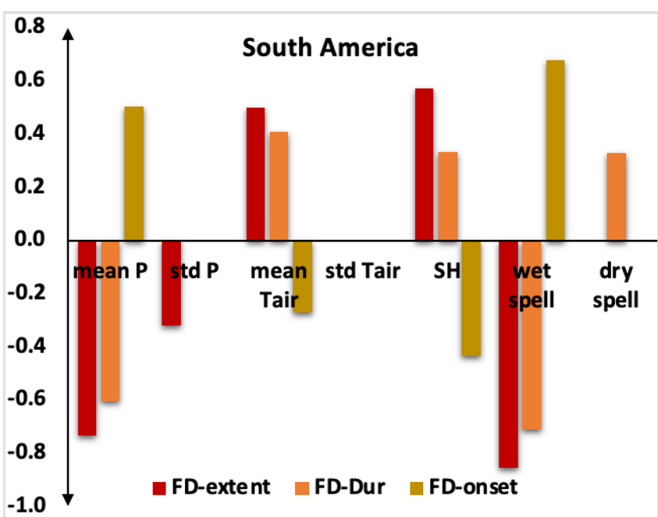
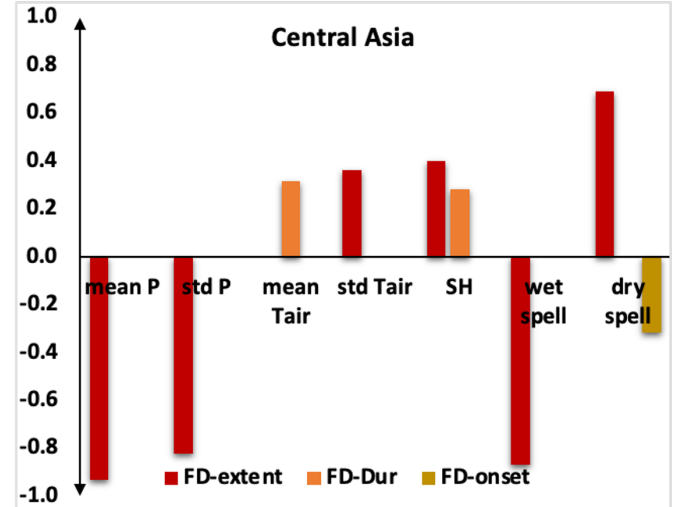
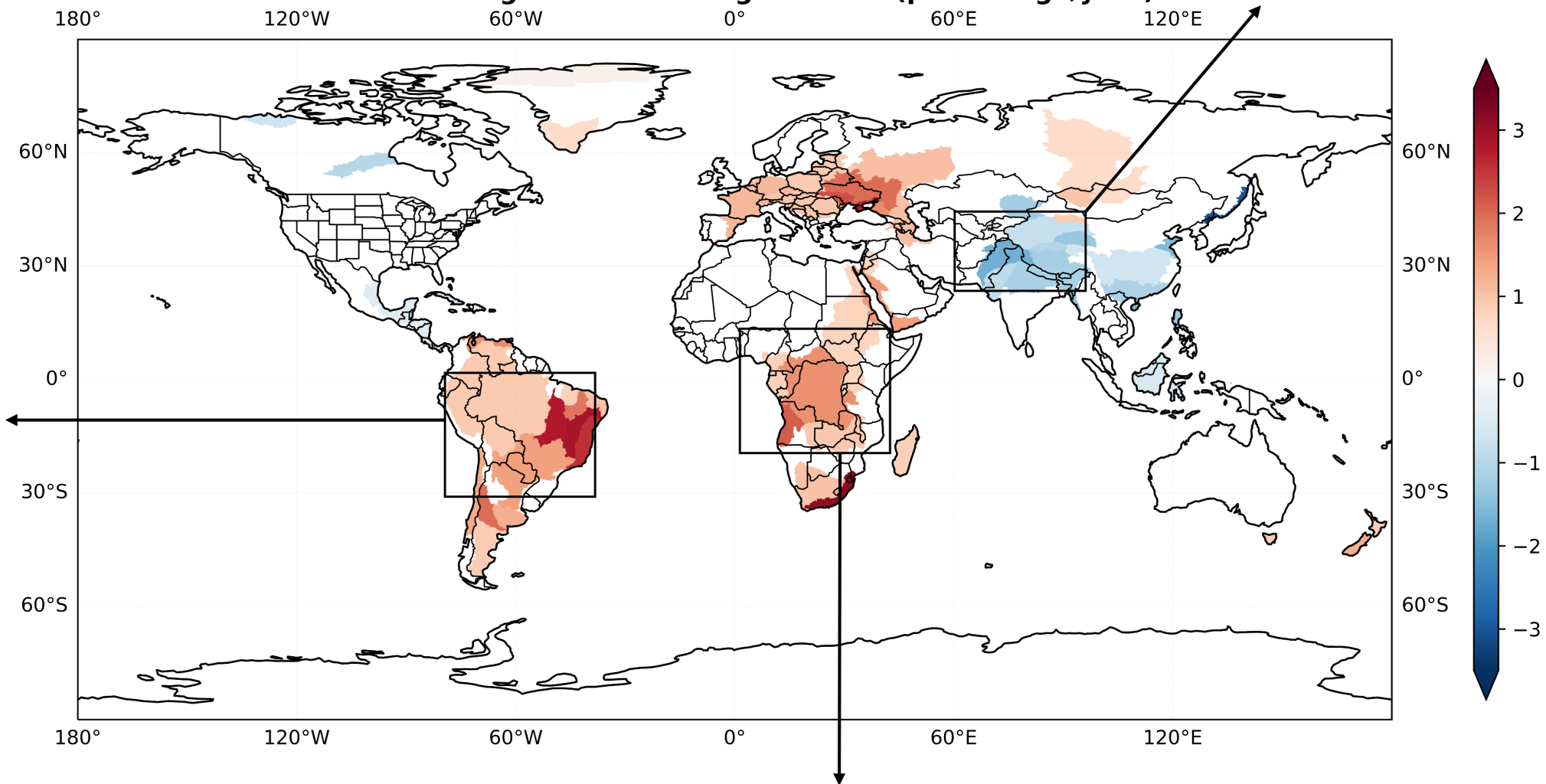
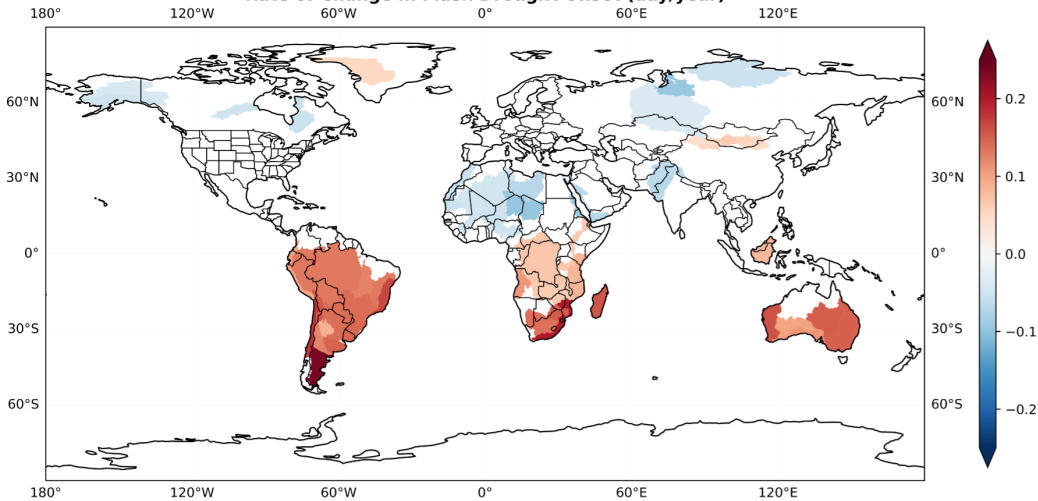


Figure2.

**Rate of Change in Flash Drought Onset (day/year)**



**Rate of Change in Flash Drought Duration (day/year)**

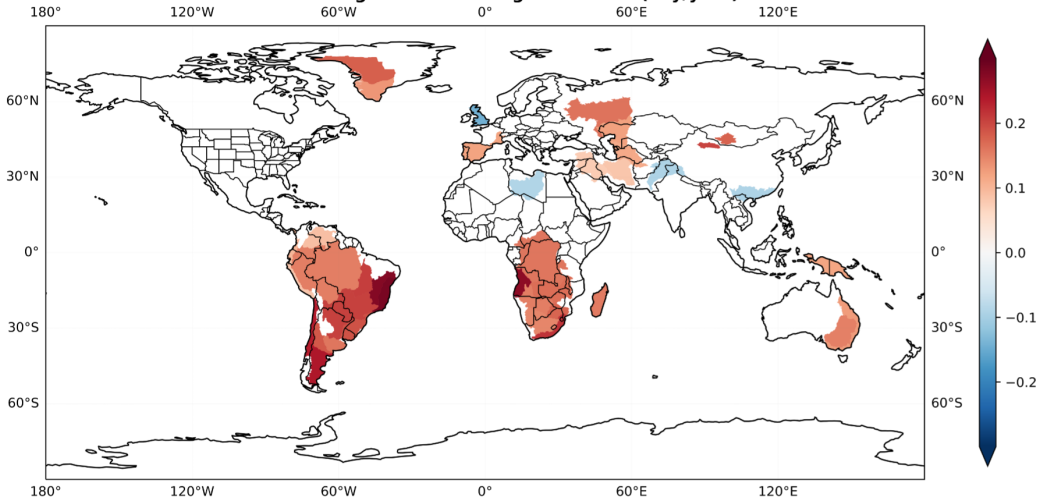


Figure3.

